CHINESE JOURNAL OF PHYSICS VOL. 41, NO. 2 APRIL 2003

Atomic Displacements in Cu due to Transition Metal Impurities

Hitesh Sharma[1] and S. Prakash[2]
[1]*Department of Physics, Panjab University, Chandigarh 160014, India*
[2]*Jiwaji University, Gwalior M.P. 474011, India*
(Received November 18, 2002)

Atomic displacements in Cu metal due to substitutional transition metal impurities are investigated using the discrete lattice model and the Kanzaki lattice static method. The effective ion-ion interaction potential, due to Wills and Harrison, is used to evaluate the dynamical matrix and the impurity-induced forces. The results for atomic displacements due to 3d, 4d and 5d impurities (Co, Ni, Pd, Ag, Pt and Au) in Cu are given up to 20 nearest impurity neighbors, and these are compared with the available experimental data; they are found to agree. The lattice shows expansion due to Co, Pd, Ag, Pt and Au impurities and contraction due to Ni impurities. The maximum displacement, 2.3% of 1NN distance, was found for the CuAu alloy, while the minimum displacements, 0.43% of 1NN distance was found for the CuNi alloy. The relaxation energies for the Ni and Pd impurities were found to be less than that of the other types of impurities, therefore these impurities may easily be solvable in Cu.

PACS. 61.72.-y – Defects and impurities in crystals; microstructure.
PACS. 61.72.Ji – Point defects (vacancies, interstitials, color centers, etc.) and defect clusters.

I. Introduction

The transition metal (TM) based alloys are technologically important. The properties of these alloys are largely influenced by their structure and the electronic nature of the host and impurity atoms. A large number of experimental techniques have been used to study the properties of these alloys. With the advance of synchrotron radiation, absorption spectroscopy has emerged as an additional tool for the study of the TM based alloys. Recent X-ray absorption fine structure (XAFS) date [1] for the transition metal based dilute alloys are of immense importance, due to a growing interest in the experimental study of these alloys. Along with the advancements in experimental techniques, the need has surfaced to study the dynamical behavior of these alloys theoretically. This would help in understanding the formation of the transition metal alloys. We used the Kanzaki lattice static method [2] to investigate the strain field due to transition metal impurities in the bcc transition metals Vanadium, Chromium, and Iron [3-5] and the fcc transition metals Nickel and Palladium [6]. The effective ion-ion interaction potential, due to Wills and Harrison [7], was used to calculate the Kanzaki forces. The calculated atomic displacements of the NN's (nearest neighbors) impurities in V, Fe, Ni, and Pd hosts exhibited the same trend as predicted by X-ray diffraction studies for the fractional change in the lattice parameters. Since the atomic displacement data calculated in the discrete lattice model are of vital importance to the study of the elastic and electronic properties of dilute alloys [8-11], a report of the calculations

for the strain field due to transition metal impurities in fcc Cu using discrete lattice model should be of interest. The plan of the paper is as follows: The necessary formalism is given in Sec. II. The calculations and results are presented in Sec. III and are discussed in Sec. IV.

II. Formalism

For a perfect crystal with a self consistent pair potential $\phi(r)$, the total interaction energy Φ_0 is given as

$$\Phi_0 = \sum_{n} \phi(\vec{R}_n^0) \tag{1}$$

where $\vec{R}_n^0$ is the equilibrium position of the nth host atom. If an impurity is introduced at the origin, the lattice becomes strained, and the host atoms move to new equilibrium positions $\vec{R}_n = \vec{R}_n^0 + \vec{u}(\vec{R}_n^0)$, where $\vec{u}(\vec{R}_n^0)$ are the atomic displacements. Kanzaki assumed that these atomic displacements are produced by an appropriate distribution of external forces in the crystal which depend upon the nature of the impurity. The potential energy of the strained lattice under applied external forces is expanded in a powers series of the displacements, which in the harmonic approximation is given as

$$\Phi = \Phi_0 - \sum_{n;\alpha} u_\alpha(\vec{R}_n^0) F_\alpha(\vec{R}_n^0) + \frac{1}{2} \sum_{n;\alpha} \sum_{n';\beta} u_\alpha(\vec{R}_n^0) u_\beta(\vec{R}_{n'}^0) \phi_{\alpha\beta}(n, n'), \tag{2}$$

where Φ_0 is the potential energy of a perfect lattice, the force components

$$F_\alpha(\vec{R}_n^0) = -\left. \frac{\partial \Phi}{\partial u_\alpha(\vec{R}_n^0)} \right|_{u_\alpha(R_n^0)=0}, \tag{3}$$

and the force constants

$$\phi_{\alpha\beta}(n, n') = \left. \frac{\partial^2 \Phi}{\partial u_\alpha(\vec{R}_n^0) \partial u_\beta(\vec{R}_{n'}^0)} \right|_{u_\alpha(R_n^0)=u_\beta(R_{n'}^0)=0}. \tag{4}$$

Here α, β (x, y, z) denote the Cartesian components. $F_\alpha(\vec{R}_n^0)$ is the α component of the external force applied on the atom R_n^0 and $\phi_{\alpha\beta}(n, n')$ are the force constants which obey the crystal symmetries. The equilibrium values of $u(R_n^0)$ are obtained by minimizing Φ with respect to $u_\alpha(R_n^0)$, i.e.

$$\frac{\partial \Phi}{\partial u_\alpha(R_n^0)} = 0. \tag{5}$$

Substituting Eq. (2) into (5), one finds

$$F_\alpha(\vec{R}_n^0) = \sum_{n';\beta} \phi_{\alpha\beta}(n, n') u_\beta(\vec{R}_{n'}^0). \tag{6}$$

Evidently the displacements can be evaluated if $F_\alpha(\vec{R}_n^0)$ and $\phi_{\alpha\beta}(n, n')$ are known.

In the Kanzaki lattice static method the displacements are expanded in normal co-ordinates as

$$u_{\alpha}(\vec{R}^0_n) = \sum_{q} Q_{\alpha}(\vec{q}) \exp(i\vec{q}.\vec{R}^0_n), \tag{7}$$

where $\vec{q}$ is a wave vector and the expansion coefficients $\vec{Q}(\vec{q})$ are normal co-ordinates. Since we are considering a periodic superlattice of defects, the wave vectors $\vec{q}$ must satisfy periodic boundary conditions, and all such physically distinct $\vec{q}$ vectors will be contained within the first Brillouin zone. $\vec{Q}(\vec{q})$ are, in general, complex and, to ensure the reality condition for displacements

$$\vec{Q}(-\vec{q}) = \vec{Q}^*(\vec{q}), \tag{8}$$

where the asterisk stands for the complex conjugate. Using Eq. (7) in Eq. (2), one gets the Fourier transform of the total energy Φ of the strained lattice:

$$\Phi = \Phi_0 + \sum_{\alpha q} F_{\alpha}(\vec{q}) Q_{\alpha}(\vec{q}) + \frac{N}{2} \sum_{\alpha\beta} \sum_{q} \phi_{\alpha\beta}(\vec{q}) Q_{\alpha}(\vec{q}) Q_{\beta}(\vec{q}), \tag{9}$$

where

$$F_{\alpha}(\vec{q}) = \sum_{n} F_{\alpha}(\vec{R}^0_n) \exp(i\vec{q}.\vec{R}^0_n), \tag{10}$$

and

$$\phi_{\alpha\beta}(\vec{q}) = \sum_{n-n'} \phi_{\alpha\beta}(n - n') \exp\left[-i\vec{q}.(\vec{R}^0_n - \vec{R}^0_{n'})\right]. \tag{11}$$

N is the number of unit cells in the crystal. $F_{\alpha}(\vec{q})$ and $\phi_{\alpha\beta}(\vec{q})$ are the Fourier transforms of $F_{\alpha}(\vec{R}^0_n)$ and $\phi_{\alpha\beta}(n - n')$, respectively. The equilibrium condition in Fourier space becomes

$$\frac{\partial \Phi}{\partial Q_{\alpha}(q)} = 0, \tag{12}$$

which in conjunction with Eq. (9) gives

$$\sum_{\beta} \left[N\phi_{\alpha\beta}(-\vec{q}) Q_{\beta}(\vec{q}) + F_{\beta}(\vec{q})\delta_{\alpha\beta}\delta_{-q;q}\right] = 0. \tag{13}$$

Equation (13) gives three simultaneous equations for three components $Q_{\beta}(\vec{q})$ for each value of $\vec{q}$. If $\phi_{\alpha\beta}(\vec{q})$ and $F_{\beta}(\vec{q})$ are known, Eq. (13) can be solved for $\vec{Q}(\vec{q})$ which, in turn, gives $u_{\alpha}(\vec{R}^0_n)$ from Eq. (7).

For a central ion-ion potential, the dynamical matrix is written as

$$\phi_{\alpha\beta}(n) = \left.\frac{\partial^2 \phi}{\partial r_{\alpha} \partial r_{\beta}}\right|_{r = R^0_n} = \frac{R^0_{n\alpha} R^0_{n\beta}}{|\vec{R}^0_n|^2}(A_n - B_n + \delta_{\alpha\beta} B_n), \tag{14}$$

where

$$A_{\mathsf{n}} = \left.\frac{\partial^2\phi}{\partial r^2}\right|_{\mathsf{r}=\mathsf{R}^0_{\mathsf{n}}}, \quad B_{\mathsf{n}} = \left.\frac{1}{\mathsf{j}\vec{R}^0_{\mathsf{n}}\mathsf{j}}\frac{\partial\phi}{\partial r}\right|_{\mathsf{r}=\mathsf{R}^0_{\mathsf{n}}}. \tag{15}$$

In the metallic crystal, the ions are screened by the conduction electrons, thereby more quuickly decreasing the ionic potential, which exhibits oscillatory behavior at large distances. It has been found that in the d-band metals the screening is large [8-10], therefore the major contribution to $\phi_{\circledR}{}^{-}(\vec{q})$ and $F_{\circledR}(\vec{q})$ in these metals is expected to arises from the first few NN's. Including the interactions up to 1NN's, $\phi_{\circledR}{}^{-}(\vec{q})$ for the fcc structure, from Eqs. (11) and (14), becomes

$$\phi_{\circledR\circledR}(\vec{q}) = 2(A_1 + B_1)\left[1 \;\mathsf{¡}\; \cos\left(\frac{q_{\circledR}a}{2}\right)\left[\cos\left(\frac{q^{-}a}{2}\right) + \cos\left(\frac{q^{\circ}a}{2}\right)\right]\right] \tag{16}$$

$$\phi_{\circledR}{}^{-}(\vec{q}) = 2(A_1 \;\mathsf{¡}\; B_1)\left[\sin\left(\frac{q_{\circledR}a}{2}\right) + \sin\left(\frac{q^{-}a}{2}\right)\right], \tag{17}$$

where α 6= β 6= γ and a is the lattice parameter. Similarly, Eq. (10) at the 1NN shell of impurity gives

$$F_{\circledR}(\vec{q}) = i2\,\mathsf{p}\overline{2}F_{\mathsf{I}}\sin\left(\frac{q_{\circledR}a}{2}\right)\left[\cos\left(\frac{q^{-}a}{2}\right)\cos\left(\frac{q^{\circ}a}{2}\right)\right], \tag{18}$$

where F_{I} is the force acting on the 1NN impurity sites. Considering the interaction with the 2NN shell, the components of $F(\vec{q})$ are

$$F_{\circledR}(\vec{q}) = i2F_{\mathsf{II}}\sin(q_{\circledR}a), \tag{19}$$

where F_{II} is the force at the 2NN impurity site.

With the knowledge of $\phi_{\circledR}{}^{-}(q)$ and $F_{\circledR}(q)$, one can solve Eq. (13) for $\vec{Q}(\vec{q})$ using the properties of determinants. For the radial forces at the 1NNs imports shell only (usually called the F_{I} system),

$$\imath Q_1(q) = \frac{\mathsf{p}\overline{2}F_{\mathsf{I}}}{NA_1}\frac{\begin{vmatrix} \sin x(\cos y + \cos z) & G_2 & G_3 \\ \sin y(\cos z + \cos x) & G_{22} & G_4 \\ \sin z(\cos x + \cos y) & G_4 & G_{33} \end{vmatrix}}{\Delta}, \tag{20}$$

where

$$\Delta = \begin{vmatrix} G_{11} & G_2 & G_3 \\ G_2 & G_{22} & G_4 \\ G_3 & G_4 & G_{33} \end{vmatrix}, \tag{21}$$

$$G_{11} = \left[1 + \frac{B_1}{A_1}\right][2 \;\mathsf{¡}\; \cos x(\cos y + \cos z)], \tag{22}$$

$$G_2 = \left[1 \;\mathsf{¡}\; \frac{B_1}{A_1}\right]\sin x \sin y, \tag{23}$$

$$G_3 = \left[1 - \frac{B_1}{A_1}\right] \sin x \sin z, \tag{24}$$

$$G_4 = \left[1 - \frac{B_1}{A_1}\right] \sin y \sin z, \tag{25}$$

$$x = \frac{q_x a}{2}, \quad y = \frac{q_y a}{2}, \quad z = \frac{q_z a}{2}. \tag{26}$$

G_{22} and G_{33} are obtained from the expression for G_{11} by the cyclic permutation of x, y, z. $Q_2(q)$ and $Q_3(q)$ can be obtained from $Q_1(q)$ using cubic symmetry. For the radial forces acting only on the 2NN impurity shell (called the F_{11} system),

$$\iota Q_1 = \frac{F_{11}}{N A_1} \begin{vmatrix} \sin 2x & G_2 & G_3 \\ \sin 2y & G_{22} & G_4 \\ \sin 2z & G_4 & G_{33} \end{vmatrix}. \tag{27}$$

$Q_2(q)$ and $Q_3(q)$ can be obtained from $Q_1(q)$ using cubic symmetry.

II-1. Calculation of F_1 and F_{11}

The external force $\vec{F}(R_n^0)$ for substitutional impurities in the fcc host is calculated considering the four configurations, as shown in Fig. 1. The difference in the potential energies of the (a) and (d) configurations is

$$\begin{aligned} \Phi(d) - \Phi(a) &= [\Phi(d) - \Phi(c)] + [\Phi(c) - \Phi(b)] + [\Phi(b) - \Phi(a)] \\ &= \sum_n [\phi_{1H}(|\vec{R}_n|) - \phi_{HH}(|\vec{R}_n|)] \\ &\quad + \frac{1}{2} \sum_{n;n'} [\phi_{HH}(|\vec{R}_{n'} - \vec{R}_n|) - \phi_{HH}(|\vec{R}^0_{n'} - \vec{R}^0_n|)], \end{aligned} \tag{28}$$

where $\phi_{HH}(r)$ and $\phi_{1H}(r)$ are the host-host and impurity-host interaction potentials respectively. Comparing Eqs. (2) and (28), we see that the second term of both expressions is the same; therefore by equating the first term of Eqs. (2) and (28), one gets

$$F_\alpha(\vec{R}_n^0) = -\frac{\partial}{\partial u_\alpha(R_n^0)} \sum_{n'} \Delta\phi(|\vec{R}_{n'}|), \tag{29}$$

where

$$\Delta\phi(r) = \phi_{1H}(r) - \phi_{HH}(r). \tag{30}$$

Expanding $\Delta\phi(|\vec{R}_{n'}|)$ in a power series of $\vec{u}(\vec{R}_n^0)$, the forces F_1 and F_{11} for the central potential are given as

$$F_\alpha(\vec{R}_n^0) = -\frac{\partial}{\partial r} \Delta\phi \,|_{|r|=|R_n^0|} - \vec{u}(\vec{R}_n^0) \frac{\partial^2}{\partial r^2} \Delta\phi \,|_{|r|=|R_n^0|}. \tag{31}$$

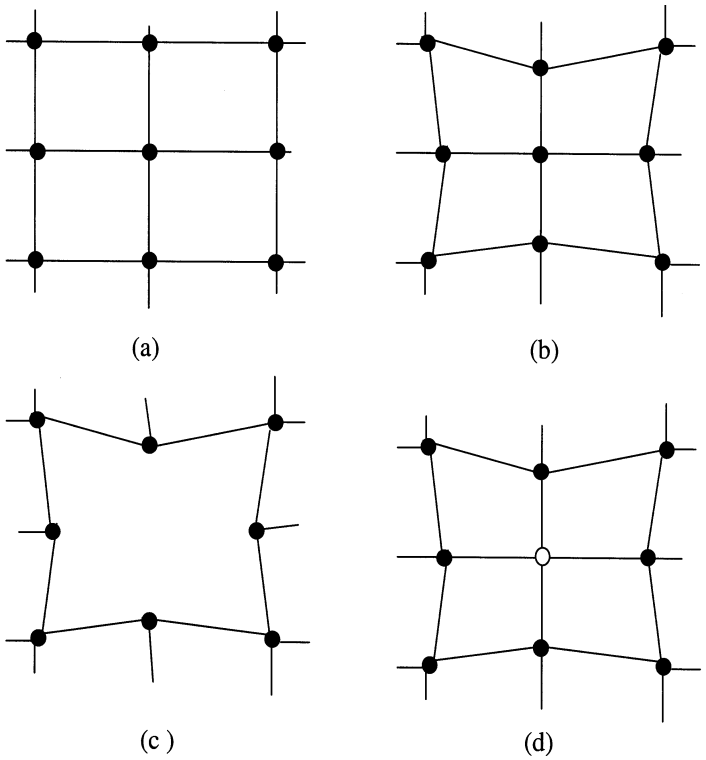

FIG. 1. The four lattice configurations for a substitutional impurity. (a) Perfect host lattice, (b) strained lattice due to an external force, (c) strained lattice with one atom removed, and (d) an impurity atom placed at the vacant lattice site.

Equation (31) can be solved with the two approximations. If $u(R_n^0)$ is very small, the second term in Eq. (31) can be neglected. The first approximation is where the force constants of the host metal remain unchanged in the presence of an impurity. If $u(R_n^0)$ is significant, both terms in Eq. (31) are retained. This is called the second approximation, and takes care of impurity-induced changes in the force constants of the lattice. To include the interactions up to 2NN's, the atomic displacements due to F_1 and F_{11} are combined to evaluate $\vec{u}(\vec{R}_n^0)$ in the second approximation, as was done by Kanzaki.

The conduction electrons in the transition metal have both an s and a quasilocalised d character, and these characteristic should be included in the calculation of the ion-ion interaction potential. In the formation of TM, the d states are broadened into quasilocalised bands with a finite bandwidth. Furthermore the d bands become distorted due to the crystal potential and there is s-d hybridization. These effects are included in the Wills and Harrison transition metal model potential [3] which is

$$\phi_{HH}(r) = \phi_{HH}^{FE}(r) + \phi_{HH}^{c}(r) + \phi_{HH}^{b}(r), \tag{32}$$

where

$$\phi^{FE}_{HH}(r) = Z^2_{sH} e^2 \cos^2(\kappa r_{cH}) \frac{\exp(-\kappa r)}{r}, \tag{33}$$

$$\phi^{c}_{HH}(r) = Z_{dH} \frac{225}{\pi^2} \frac{\hbar^2 r^6_{dH}}{m r^8}, \tag{34}$$

and

$$\phi^{b}_{HH}(r) = -Z_{dH} \left[1 - \frac{Z_{dH}}{10}\right] \left[\frac{12}{n}\right]^{1/2} \frac{28.1}{\pi} \frac{\hbar^2 r^3_{dH}}{m r^5}. \tag{35}$$

Here $\phi^{FE}_{HH}(r)$ is the free electron contribution, $\phi^{c}_{HH}(r)$ arises from the shift in the d band center due to the s-d hybridization and ϕ^{b}_{HH} arises from the finite d-bandwidth. Z_{sH} and Z_{dH} are the number of s and d conduction electrons per host atom, κ is the Thomas Fermi screening constant, r_{cH} is the Ashcroft model-potential core radius and r_{dH} is the d state radii. n is the number of 1NNs in the host lattice and m is the mass of the electron.

Equations (32)-(35) are generalized to produce the interatomic potential for the impurity -host interaction in the dilute alloys, which is [3]

$$\phi_{IH}(r) = \phi^{FE}_{IH}(r) + \phi^{c}_{IH}(r) + \phi^{b}_{IH}(r), \tag{36}$$

where

$$\phi^{FE}_{IH}(r) = Z_{sH} Z_{sI} e^2 \cos(\kappa^0 r_{cH}) \cos(\kappa^0 r_{cI}) \frac{\exp(-\kappa^0 r)}{r} \tag{37}$$

$$\phi^{c}_{IH}(r) = Z^{eff}_{d} \frac{225}{\pi^2} \frac{\hbar^2 r^3_{dH} r^3_{dI}}{m r^8} \tag{38}$$

and

$$\phi^{b}_{IH}(r) = -Z^{eff}_{d} \left[1 - \frac{Z^{eff}_{d}}{10}\right] \left[\frac{12}{n}\right]^{1/2} \frac{28.1}{\pi} \frac{\hbar^2 r^{3/2}_{dH} r^{3/2}_{dI}}{m r^5}. \tag{39}$$

Here Z_{sI} and Z^{eff}_{d} are the number of s conduction electrons and the effective quasilocalized d-electron per impurity atom. In Eq. (38) r_{dI} is the d-state radius, r_{cI} is the Ashcroft model-potential core radius for the impurity and κ^0 is the Thomas Fermi screening length for the host-impurity interaction. It is difficult to know the variation in the number of d electrons in the d-band introduced by the introduction of an impurity. Therefore we take the effective number of d electrons, Z^{eff}_{d}, in an alloy as the weighted average of the number of d electrons in the host and impurity atoms, i.e.

$$Z^{eff}_{d} = C_H Z_{dH} + C_I Z_{dI}, \tag{40}$$

where Z_{dI} is the number of quasilocalized d electrons per impurity atom and C_H and C_I are the concentrations of host and impurity atoms respectively.

In the alloying process, there may be a further transfer of electrons to or from the s and d bands, as a result of which the conduction electron charge would redistribute around any impurity

to screen or unscreen it. However we assume that these charge transfers are small, so we can write the excess interatomic potential due to the impurity as

$$\Delta\phi(r) = \Delta\phi^{FE}(r) + \Delta\phi^{c}(r) + \Delta\phi^{b}(r), \tag{41}$$

where

$$\Delta\phi^{FE}(r) = \frac{Z_{sH}\,e^2}{r} \left[Z_{sI}\cosh(\kappa^{0} r_{cH})\cosh(\kappa^{0} r_{cI})\exp(-\kappa^{0} r) - Z_{sH}\cosh^2(\kappa r_{cH})\exp(-\kappa r) \right], \tag{42}$$

$$\Delta\phi^{c}(r) = \left[Z_{d}^{eff} r_{dI}^3 - Z_{dH} r_{dH}^3 \right] \frac{225}{\pi^2} \frac{\sim^2 r_{dH}^3}{m r^8}, \tag{43}$$

and

$$\Delta\phi^{b}r) = \left[-Z_{d}^{eff} \left(1 - \frac{Z_{d}^{eff}}{10}\right) r_{dI}^{3=2} + Z_{dH}\left(1 - \frac{Z_{dH}}{10}\right) r_{dH}^{3=2} \right] \left[\frac{12}{n}\right]^{1=2} \frac{28.1}{\pi} \frac{\sim^2 r_{dH}^{3=2}}{m r^5}. \tag{44}$$

In Eqs. (41) to (44), $\Delta\phi^{FE}(r)$, $\Delta\phi^{c}(r)$ and $\Delta\phi^{b}(r)$ are impurity induced changes in the potential due to the free electrons, s-d hybridization and d-band width contributions, respectively.

III. Calculations and results

The above formalism is used to calculate the atomic displacements in Cu dilute alloys due to 3d (Co and Ni), 4d (Pd and Ag) and 5d (Pt and Au) transition metal impurities. The physical parameters and a few of the calculated results are given in Tables I and II. The host potential $\phi_{HH}(r)$ and the impurity host potential $\phi_{IH}(r)$ are used to calculate the excess potential $\Delta\phi(r)$ using Eq. (41).

The change in potential $\Delta\phi(r)$ due to impurities in Cu metal depends upon the impurity induced s-d hybridization and a shift in the d band center which depends on the difference between the Ashcroft core radius and the d-state radius of the impurity and the host. In the dilute alloys of Cu, $\Delta\phi(r)$ for the 3d impurities is smaller by an order of magnitude than for the 4d and 5d impurities. $\Delta\phi(r)$ is repulsive at small distances but becomes attractive at large distances for all the impurities.

TABLE I. The physical parameters (in a.u.) of Cu metal. a is the lattice parameter, Ω_0 is the atomic volume, Z is number of s and d conduction electrons per atom and A_1, B_1 are the force constants as defined in Eq. 15.

Host	a	Ω_0	Z	A_1 (10^{-2})	B_1 (10^{-2})
Cu	6.82	76	11	1.5669	-0.3474

TABLE II. r_c and r_d are the Ashcroft core radius and d state radius respectively, F_I and F_{II} (in a.u.) are impurity-induced forces evaluated at 1NN's and 2NN's in the second approximation, and E_r is the relaxation energy.

Imp.	Cu				
	r_c (a.u.)	r_d (a.u.)	F_I (10^{-3})	F_{II} (10^{-3})	E_r $(-10^{-3}$ eV)
Co	1.55	1.70	3.52	0.21	1.94
Ni	1.00	1.34	1.47	0.08	0.35
Cu	0.87	1.27			
Pd	0.98	1.77	5.83	0.18	0.52
Ag	0.85	1.68	6.10	0.31	5.83
Pt	0.62	1.97	6.67	0.11	7.03
Au	0.76	1.91	7.78	0.36	9.49

The calculated $\Delta\phi(r)$ is used in Eq. (31) to calculate F_I and F_{II} at the 1NN and 2NN impurity in the second approximation. The F_I and F_{II} values which are sensitive to the slope of $\Delta\phi(r)$ are given in Table II. In the Cu host, the forces are repulsive at 1NN's and 2NN's for Co, Pd, Ag, Pt and Au impurities. For an Ni impurity the forces are attractive at the 1NN's and repulsive at the 2NN's.

These values of F_I and F_{II}, and the calculated values of the force constants A_1 and B_1, are used to calculate $\phi_{\alpha\alpha}(\vec{q})$, and hence $\vec{Q}(\vec{q})$, with the help of Eqs. (20-27). The inverse Fourier transform of $\vec{Q}(\vec{q})$, as given in Eq. (7) gives $\vec{u}(\vec{R}_n^0)$. The numerical calculations are simplified by replacing the sum over $\vec{q}$ by the integration over the cube of edge $4\pi/a$, which inscribes the first Brillouin zone, and using the fact that for any function $F(q)$,

$$\int_{BZ} F(q)dq = \frac{1}{2}\int_{cube} F(q)dq, \tag{45}$$

for the fcc structure. The integration is carried out by a Gaussian quadrature method. The calculated values of atomic displacements are tabulated in Tables III to V for Cu(Co, Ni, Pd, Ag, Pt and Au) dilute alloys, respectively. These displacements are oscillatory in nature and are significant even up to twenty nearest neighbors of impurity which are tabulated here.

In the CuCo dilute alloy the 1NN's are displaced away from the impurity, one the 2NN's are displaced towards impurity atom, and the third and fourth NN's are displaced away from the impurity, which are followed by an oscillatory nature of displacements. The maximum $|u(r)|$ due to Co is found at the 1NN's site. For the Co impurity, the number of atoms displaced away from

TABLE III. Atomic displacements (in a.u.) of the NN's for Co and Ni impurities in Cu. The coordinates (n_1, n_2, n_3) of the NN's are in units of (a/2) and (u_x, u_y, u_z) are the cartesian components of the atomic displacements here and also in the subsequent tables.

NN's (n_1, n_2, n_3)	Co			Ni		
	u_x	u_y	u_z	u_x	u_y	u_z
110	0.0353	0.0353	0.0000	-0.0150	-0.0150	0.0000
200	-0.0078	0.0000	0.0000	0.0080	0.0000	0.0000
211	0.0106	0.0118	0.0118	-0.0043	-0.0051	-0.0051
220	0.0164	0.0164	0.0000	-0.0070	-0.0070	0.0000
310	-0.0067	0.0016	0.0000	0.0038	0.0002	0.0000
222	0.0109	0.0109	0.0109	-0.0047	-0.0047	-0.0047
321	0.0063	0.0078	0.0048	-0.0026	-0.0032	-0.0019
400	-0.0075	0.0000	0.0000	0.0029	0.0000	0.0000
411	-0.0052	-0.0004	-0.0004	0.0025	0.0005	0.0005
330	0.0090	0.0090	0.0000	-0.0039	-0.0039	0.0000
420	-0.0027	0.0010	0.0000	0.0015	0.0000	0.0000
332	0.0076	0.0076	0.0060	-0.0032	-0.0032	-0.0024
422	0.0030	0.0034	0.0034	-0.0011	-0.0012	-0.0012
431	0.0041	0.0050	0.0018	-0.0017	-0.0020	-0.0007
510	-0.0044	-0.0009	0.0000	0.0016	0.0004	0.0000
521	-0.0032	-0.0006	-0.0005	0.0015	0.0004	0.0003
440	0.0056	0.0056	0.0000	-0.0024	-0.0024	0.0000
433	0.0054	0.0049	0.0049	-0.0022	-0.0020	-0.0020
530	-0.0008	0.0009	0.0000	0.0005	-0.0002	0.0000
442	0.0051	0.0051	0.0028	-0.0021	-0.0021	-0.0011

TABLE IV. Atomic displacements (in a.u.) of the NN's of Pd and Ag impurities in Cu.

NN's (n_1, n_2, n_3)	Pd			Ag		
	u_x	u_y	u_z	u_x	u_y	u_z
110	0.0588	0.0588	0.0000	0.0613	0.0613	0.0000
200	-0.0177	0.0000	0.0000	-0.0152	0.0000	0.0000
211	0.0174	0.0198	0.0198	0.0183	0.0205	0.0205
220	0.0273	0.0273	0.0000	0.0284	0.0284	0.0000
310	-0.0121	0.0017	0.0000	-0.0119	0.0024	0.0000
222	0.0182	0.0182	0.0182	0.0190	0.0190	0.0190
321	0.0103	0.0128	0.0078	0.0108	0.0134	0.0083
400	-0.0122	0.0000	0.0000	-0.0129	0.0000	0.0000
411	-0.0090	-0.0010	-0.0010	-0.0092	-0.0008	-0.0008
330	0.0150	0.0150	0.0000	0.0156	0.0156	0.0000
420	-0.0049	0.0012	0.0000	-0.0049	0.0015	0.0000
332	0.0127	0.0127	0.0098	0.0132	0.0132	0.0103
422	0.0049	0.0054	0.0054	0.0052	0.0058	0.0058
431	0.0068	0.0083	0.0029	0.0071	0.0087	0.0031
510	-0.0070	-0.0016	0.0000	-0.0075	-0.0016	0.0000
521	-0.0054	-0.0011	-0.0009	-0.0055	-0.0010	-0.0008
440	0.0094	0.0094	0.0000	0.0098	0.0098	0.0000
433	0.0089	0.0080	0.0080	0.0094	0.0084	0.0084
530	-0.0015	0.0013	0.0000	-0.0014	0.0015	0.0000
442	0.0084	0.0084	0.0045	0.0088	0.0088	0.0048

TABLE V. Atomic displacements (in a.u.) of the NN's for Pt and Au impurities in Cu.

NN's (n_1, n_2, n_3)	Pt			Au		
	u_x	u_y	u_z	u_x	u_y	u_z
110	0.0674	0.0674	0.0000	0.0782	0.0782	0.0000
200	-0.0229	0.0000	0.0000	-0.0202	0.0000	0.0000
211	0.0198	0.0227	0.0227	0.0233	0.0262	0.0262
220	0.0313	0.0313	0.0000	0.0363	0.0363	0.0000
310	-0.0144	0.0015	0.0000	-0.0154	0.0029	0.0000
222	0.0210	0.0210	0.0210	0.0242	0.0242	0.0242
321	0.0118	0.0145	0.0089	0.0138	0.0171	0.0105
400	-0.0138	0.0000	0.0000	-0.0164	0.0000	0.0000
411	-0.0105	-0.0013	-0.0013	-0.0118	-0.0011	-0.0011
330	0.0172	0.0172	0.0000	0.0199	0.0199	0.0000
420	-0.0058	0.0011	0.0000	-0.0063	0.0019	0.0000
332	0.0145	0.0145	0.0112	0.0169	0.0169	0.0132
422	0.0055	0.0061	0.0061	0.0066	0.0073	0.0073
431	0.0078	0.0094	0.0033	0.0091	0.0111	0.0040
510	-0.0079	-0.0019	0.0000	-0.0095	-0.0021	0.0000
521	-0.0062	-0.0014	-0.0011	-0.0071	-0.0014	-0.0011
440	0.0108	0.0108	0.0000	0.0124	0.0124	0.0000
433	0.0102	0.0091	0.0091	0.0120	0.0107	0.0107
530	-0.0018	0.0014	0.0000	-0.0019	0.0019	0.0000
442	0.0096	0.0096	0.0051	0.0112	0.0112	0.0061

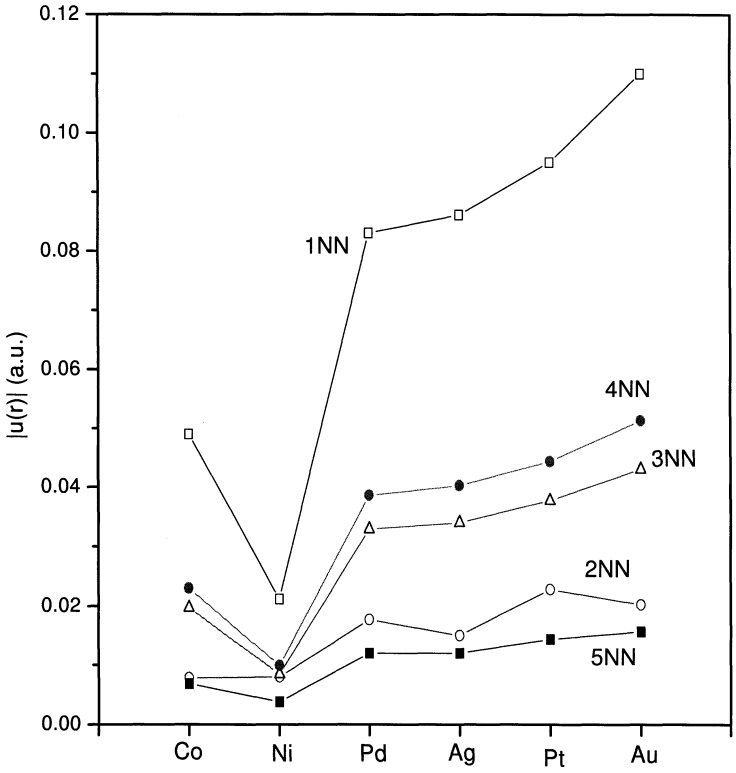

FIG. 2. The atomic displacements of the 5NN's for the Co, Ni, Pd, Ag, pt, and Au impurities in Cu host. The solid joining lines are for visual guidance.

the impurity are larger than those that move towards the impurity atom. In CuNi the (310), (321) and (411) NN's show both the anisotropic displacements and atomic displacements due to the Ni impurity. For the Ni impurity the displacements of NN's which move towards the impurity are larger then those which move away from the impurity, therefore the lattice contracts. The The displacements due to Pd, and Ag impurities are isotropic as well as anisotropic. The j$u(r)$j is maximum at 1NN's and the behavior of NN's is similar to that of the Co impurity. The behavior of the Pt and the Au impurities is similar to that of the Pd and Ag impurities. The maximum displacement occurs at the 1NN and is directes away from the impurity.

The magnitude of atomic displacements for Cu alloys up to 5NN's are shown in Fig. 2. The strain field decreases with the increase in the d-electrons for 3d impurities, i.e. from Co to Ni. For 4d impurities also the strain increases from the Pd to the Ag impurity. A similar trend is found for the strain field due to 5d impurities Pt and Au. The maximum displacement of 2.3% of R_1^0 is found for the CuAu alloy while the minimum displacement of 0.43% of R_1^0 occurt for the CuNi alloy.

The calculated atomic displacement of the 1NN's for Pd, Ag, Pt and Au impurities in Cu show a lattice expansion of 0.0832 a.u., 0.0867 a.u., 0.0953 a.u and 0.11057 a.u. at 1NN's, whereas corresponding experimental observations show lattice expansions of 0.0718 § 0.0076 au.,

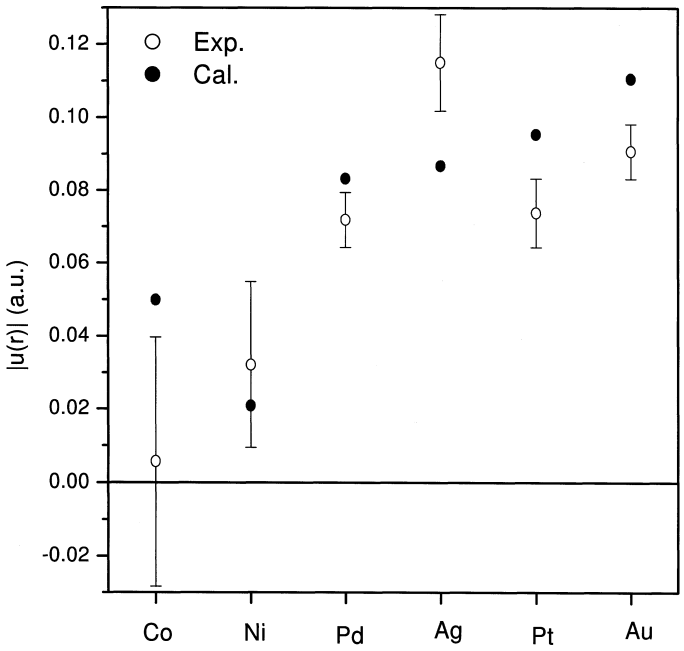

FIG. 3. The magnitude of the displacement j$u(r)$j compared with the experimental value for the Co, Ni, Pd, Ag, Pt, and Au impurities in Cu.

0.115 § 0.0132 a.u., 0.0737 § 0.00945 a.u. and 0.0907 § 0.0076 a.u., respectively [1]. The calculated $u(r)$ at 1NN due to a Ni impurity shows a contraction of 0.0208 a.u. at 1NN's while the experimental results showed a contraction of 0.0321 § 0.023 at 1NN's [1]. For the Co impurity calculated $u(r)$ gives an expansion of 0.0499 a.u. at 1NN's, whereas the experimental value at 1NN's is 0.00567 § 0.034 (i.e. varies from the contraction of 0.028 a.u. to expansion of 0.0397 a.u..) [1]. Due to large error bars in the experimental values as shown in Fig. 3, the exact comparison remains inconclusive. The calculated and experimental results however are in good qualitative agreement.

The calculated atomic displacements up to 2NN's are used to calculate the impurity induced relaxation energy E_{r}, which is given as

$$E_{\mathrm{r}} = \mathrm{i}\,\frac{1}{2}\sum_{\mathrm{n}®} F_{\mathrm{n}®} u_{\mathrm{n}®}. \tag{46}$$

Here $\vec{F}$ is isotropic; the values of F_{l} and $F_{\mathrm{l\,l}}$ tabulated in Table II are used in Eq. (46). The results for E_{r} are also given in Table II. The relaxation energies for Ni, and Pd are smaller than for other impurities, therefore these impurities may be easily dissolved in Cu. However in the case of Pt and Au, the relaxation energies are larger than other impurities, and these may not easily be dissolved in Cu.

IV. Discussion

We have used here, the Wills and Harrison model potential [7] for the host Cu metal and the other transition metal impurities. The effect of partially localized d-electrons is included through a d band width and s-d hybridization. The host potential $\phi_{HH}(r)$ and the change in potential due to the impurity $\Delta\phi(r)$ are very small and smooth beyond the 2NN distance, therefore the contribution to $\phi_{®^-}(q)$ and $F_{®}(q)$ are expected to be small beyond 2NN's. In the present calculations, it is assumed that the impurity is screened by Fermi-Thomas screening, therefore Fridel oscillations are absent. In the numerical calculations the cubic symmetry of the lattice is retained, although the exact anisotropy of the Brillouin Zone is not accounted for. This may not introduce serious errors considering other simplifications in the calculations.

The displacements compared with the XAFS results, shows that the calculated displacements are in close qualitative agreement with the experimental values, considering the error bars in the calculations. The d charge of the dilute alloys has been approximated as an effective charge in our calculations, as it is always difficult to estimate the transfer the d charge in transition metal based alloys. A more accurate effective d charge value would certainly improve the atomic displacements. The tabulated displacements values may be quite useful for investigation of the heat of solution, electric field gradients, asymmetry parameter, wipe out number, Knight shift, and other properties of the defect lattice, where impurity induced displaced positions of the host atoms in dilute alloys of Cu are needed. This will help in our basic understanding of alloy formation. Furthermore this study will explain the strength at a high temperature, the high stiffness, the low coefficient of thermal expansion, and the chemical compatibility in a variety of environments.

Acknowledgment

The financial support from the University Grant Commission (UGC), New Delhi is gratefully acknowledged.

References

[1] U. Scheuer and B. Lengeler, Phys. Rev. **B44**, 9883 (1991).
[2] H. Hanzaki, J. Phys. Chem. Solids, **2**, 24 (1957).
[3] J. Singh, P. Singh, S. K. Rattan and S. Prakash, Phys. Rev. **B49**, 932 (1994).
[4] Hitesh Sharma and S. Prakash, Pramana : J. of Phys, **59(3)**, 497 (2002).
[5] Hitesh Sharma and S. Prakash, Canadian J. of Phys. 2002 (in press).
[6] Hitesh Sharma and S. Prakash, Pramana : J. of Phys. **60(1)**, 123 (2003).
[7] J. M. Wills and W. A. Harrison, Phys. Rev. **B28**, 4363 (1983).
[8] P. Singh, S. Prakash and J. Singh, Phys. Rev. **B49**, 12259 (1994).
[9] A. Gordon and S. Dorfman, Phys. Rev. **B51**, 930 (1995).
[10] D. Fucks and S. Dorfman, Phys. Rev. **B55**, 3461 (1997).
[11] P. Singh and S. Prakash, Phys. Rev. **B59**, 14226 (1999).
[12] W. Hanke, Phys. Rev. **B8**, 4585 (1973); 4591(1973).
[13] J. Singh, N. Singh and S. Prakash, Phys. Rev. **B12**, 3159 (1975), **12**, 3166 (1975); **18**, 2954 (1978).
[14] J. Singh and S. Prakash, Nuovo Cimento **37**, 131 (1977).